Multidiszciplináris Tudományok, 15. kötet, 4. sz. (2025) pp. 32–40. ***https://doi.org/10.35925/j.multi.2025.4.3***

AN INVESTIGATION INTO THE EVOLUTION OF THE DEFORMATION STATE IN SINGLE POINT INCREMENTAL FORMING

Marwen Habbachi
PhD student, Institute of Applied Mechanics, University of Miskolc
3515 Miskolc-Egyetemváros, e-mail: marwen.habbachi@student.uni-miskolc.hu

Attila Baksa
associate professor, Institute of Applied Mechanics, University of Miskolc
3515 Miskolc-Egyetemváros, e-mail: attila.baksa@uni-miskolc.hu

Abstract

Single point incremental sheet metal forming (SPIF) is a novel and flexible forming technology that has been emerged and spread its application for the production of various customized sheet metal parts. This alternative of incremental sheet metal forming (ISF) has gained a good reputation compared to the traditional forming methods in case of low production volume. However, the deformation state is still unclear in the different part regions. Therefore, in the current investigation, a finite element analysis has been devoted to study the evolution of the stress triaxiality during the SPIF process of pure aluminium alloy Al 1050. The triaxial state has strong dependence on the located cone-forming regions indicating a dominate stress state.

Keywords: *Numerical modelling, single point incremental forming (SPIF), deformation state, localized deformation, Al 1050*

1. Introduction

Single point incremental sheet metal forming process (SPIF) has attracted considerable attention for forming metal components without the need for dedicated tooling (Emmens et al., 2010). This makes SPIF highly suitable for producing customized products, small-volume series, and rapid prototyping, which make the process welcomed (Dakhore et al., 2022; Habbachi & Baksa, 2024; Jeswiet et al., 2005). The elaboration of this technique increased the forming sector flexibility such as the manufacturing of single-use parts in the medical implants (Bensaid et al., 2023). In contrast, conventional sheet metal forming processes such deep drawing and stamping are typically recommended only for high-volume production rate due to their reliance on sophisticated tooling. Moreover, SPIF offers advantages such as simple implementation, high flexibility, and reduced com giving it several advantages over traditional forming technique (Kumar & Maji, 2021; Maaß et al., 2022; Racz et al., 2018). Consequently, it has garnered significant attention from the engineering community (Ambrogio et al., 2012). This innovative technique involves incrementally forming a clamped sheet metal blank along its periphery by moving a stylus-shaped forming tool along a predefined toolpath in a spatial coordinate system (x, y, z, t) as shown in *Figure 1*, generally controlled by a CNC machine or a dedicated robot (Sasso et al., 2008; Vihtonen et al., 2008). The improved formability of the this alternative with relative to the conventional forming technologies is mainly attributed to the localized deformation that arises when the tool deform the sheet layer by layer (Guo et al., 2013; Park & Kim, 2003). (Shrivastava & Tandon, 2019) reported

that the formability in SPIF has been improved owing to the change of texture evolution from cube-type to brass and P-type textures during the forming process. Additionally, it was found, that the plane strain state accompanied by through-thickness shear (TTS), particularly in the sidewall of the formed part, significantly influences the deformation behaviour in SPIF. Furthermore, the review by (Ai & Long, 2019) has examined to reason behind the formability in ISF process, and proposed a possible explanation of the fracture mechanism phenomenon observed in both SPIF and double-sided incremental forming (DSIF) processes. Their study revealed that stress triaxiality strongly affects material formability and the fracture bahavior in ISF. As the deformation mechanism and the stress state are more complex and strongly depend on the loading condition. Therefore, the current investigation is intended to study the evolution of the state of deformation through the evaluation of the strain in single point incremental forming of commercial pure aluminum alloy Al 1050 through both numerical analysis and experimental investigation.

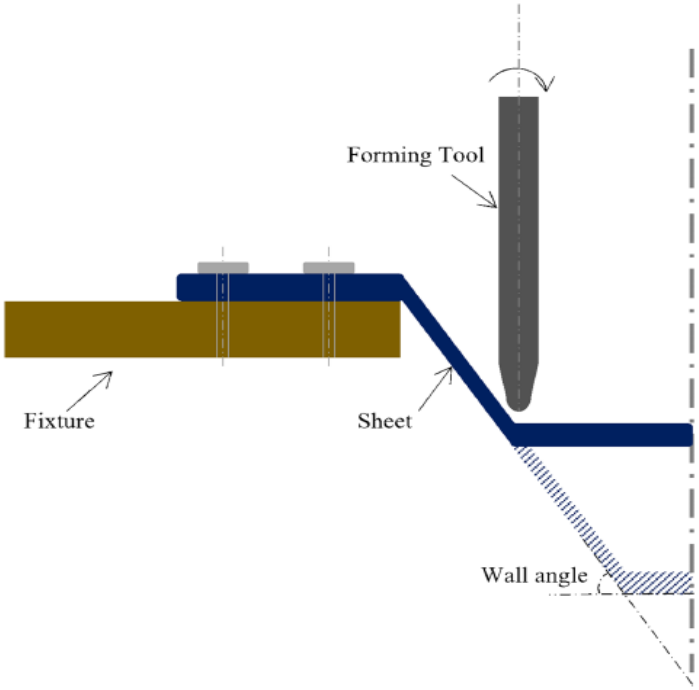

Figure 1. *Schematic of single point incremental sheet metal forming mechanism* (Dewangan et al., 2025)

2. Materials and methods

This section aims to present the experimental setup and the numerical model during the single point incremental sheet forming of pure aluminium alloy Al 1050.

2.1. Material characterization of Al 1050

A uniaxial tensile test based on the ASTM E-8 was conducted on MTS tensile testing machine to determine the mechanical properties of the aluminium alloy sheet with an initial thickness of 1 mm. Aluminium was selected due to its excellent strength-to-weight ratio, higher ductility, corrosion

resistance, and highly reflective finish. These characteristics make it a preferred material for a wide range of general applications. *Table 1* presents the chemical composition of this aluminium alloy grade, providing insights into its elemental makeup and ensuring a comprehensive understanding of its material properties. The material exhibit an ultimate strength R_m of approximately 155 MPa, and a proof yielding of $\sigma_y = 92.5$ MPa, the material exhibits considerable strength while maintaining a high level of ductility. Based on a 50 mm initial gage, the elongation at break of this material reaches 6.9%. Additionally, the elastic modulus of the material is measured to be $E = 69.5$ GPa, indicating its ability to deform under stress while returning to its original shape once the stress is removed. The Poisson's ratio is calculated to be 0.33. The true stress-strain curve is illustrated in *Figure 2*.

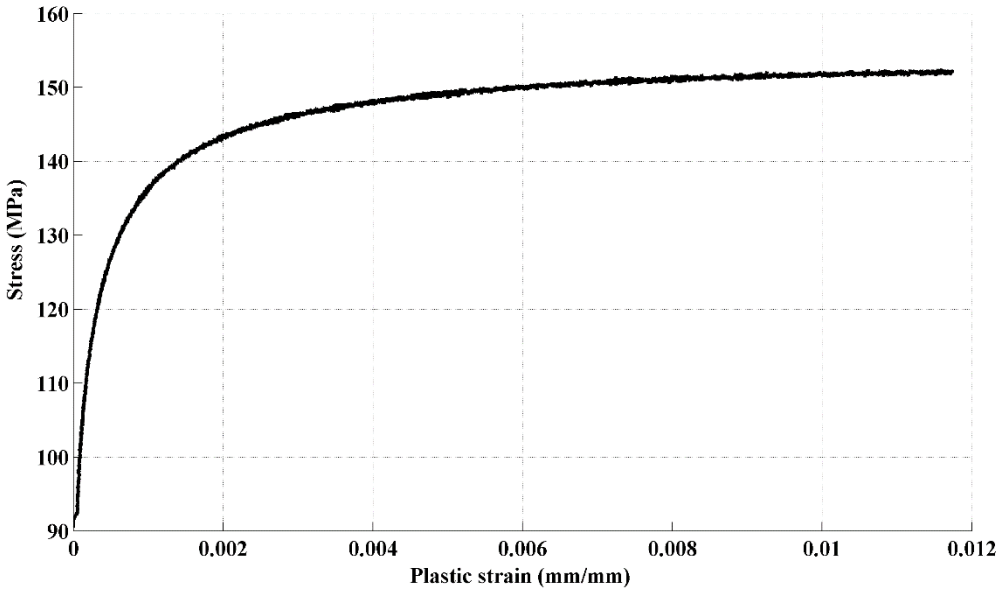

Figure 2. *True stress-plastic strain curve*

The Lankford anisotropy coefficients of the sample sheets were considered in the numerical simulations, as presented in *Table 2*. These coefficients provide crucial insights into the material's directional deformation behaviour, allowing for a more accurate representation of its response forming processes. By incorporating these detailed material properties and parameters into our investigation, the accuracy and reliability of the numerical simulations were significantly improved, providing a valuable insights into the behaviour of Al 1050 aluminium alloy during the SPIF process.

Table 1
Chemical composition of Al 1050

Element	Si	Fe	Cu	Mn	Mg	Zn	Ti	Al
Weight (%)	0.25	0.4	0.05	0.05	0.05	0.07	0.05	99.5

Table 2
Anisotropy coefficients of Al 1050

Anisotropy coefficients	r_0	r_{45}	r_{90}
Values	1.59	1.28	1.3

3. Tool path generation

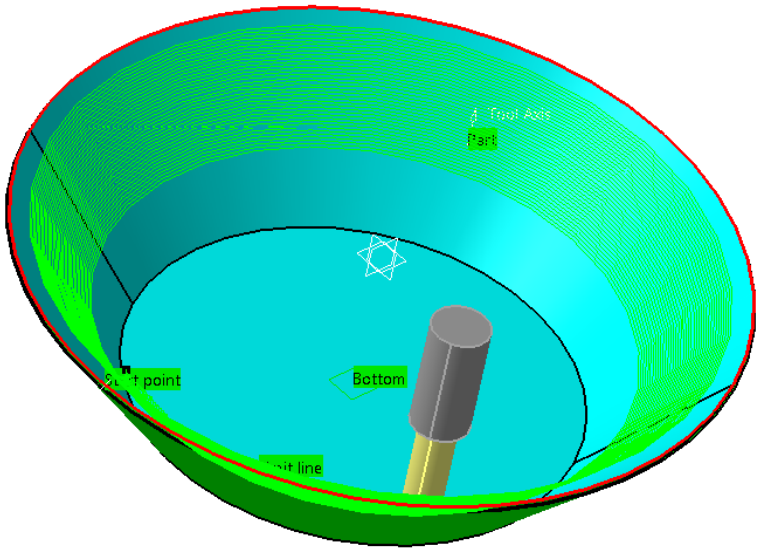

Figure 3. *Profile toolpath with standard process parameters*

In this section, the toolpath was generated to coordinate the tool movement. A profile trajectory with standard process parameters was employed. The tool diameter was set to $d = 10$ mm, the step size to $\Delta z = 0.6$ mm, the wall angle was fixed at $\psi = 60°$, the feed rate at $F = 2000$ mm/min, and the drawing height equal to $h = 43.3$ mm. The use of a profile trajectory has been associated with lower surface quality compared to the spiral toolpath, as reported by (Jeswiet et al., 2005). However, it offers a shorter forming time, highlighting its efficiency in achieving desired forming outcomes. To accurately implement this toolpath, we utilized CATIA was used a CAD software equipped with an integrated CAM package, which enabled seamless generation of coordinates (x, y, z) required to guide the forming tool's movements. *Figure 3* provides a visual representation of the programmed toolpath, illustrating the prescribed process parameters and the trajectory followed by the forming tool. This graphical depiction provides a clear insight into the planned sequence of movements and helps to understand how the chosen toolpath influences the deformation process.

4. Numerical modeling of SPIF

A finite element analysis was conducted to assess the single-point incremental sheet metal forming of an aluminum alloy sheet Al 1050. The Abaqus Explicit package has been selected for this investigation, taking into account material nonlinearities and substantial deformation inherent in the process. The sheet is represented as a deformable body with dimensions of 1 mm thickness and a $200 \times 200\ \text{mm}^2$ square sheet, while the forming tool and the backing plate are modelled as rigid bodies. A lubrification has been used during the experimental investigation which prove to adopt a friction coefficient $f = 0.05$ to model the interactions between the tools and the sheet at the interface. An assembly model is depicted in *Figure 4*.

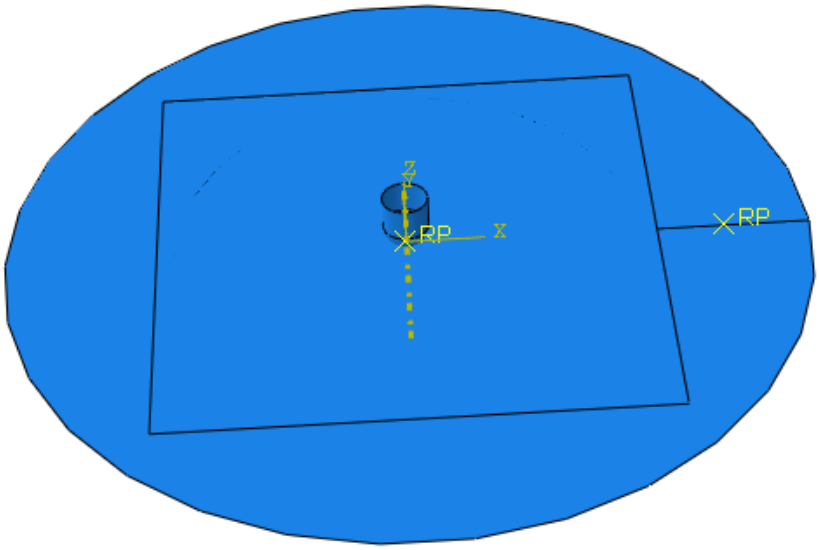

Figure 4. *Assembly model of SPIF process*

4.1. Boundary conditions

The entire model was carried numerically to be close replicate the real experimental setup. To simulate practical constraints, the element located along the sheet periphery were clamped at their edges. A displacement along x, y, and z axes was applied to the forming tool, guiding its movement along the (x, y) plane at each contour, while a specific step depth (Δz) controlled its downward motion.

To execute these complex movements, a predefined toolpath has been generated using Computer-Aided Manufacturing (CAM) package. The CAM package facilitated the programming of tool movements in the x, y, and z directions, ensuring seamless coordination between the virtual representation of the forming tool and the numerical simulation environment.

By employing this integrated approach, It was able to accurately replicate the dynamic interactions between the forming tool and the workpiece, capturing the complex mechanical behavior inherent in the single-point incremental forming (SPIF) process. This enabled the generation of reliable data and insights into the behaviour of forming forces, stress distribution, and deformation patterns, contributing to a deeper understanding of SPIF and its optimization for practical applications.

5. Results and discussions

The forming force evolution in single-point incremental forming (SPIF) is different from the conventional sheet metal forming, which mainly influenced by the process parameters and process condition. As this is a complex process influenced by various process parameters that have an impact on the forming force, surface quality, and stress distribution. Forming forces F_x, F_y, and F_z were evaluated numerically as depicted in *Figure 5*. The axial forming force in the steady-state regime was compared with the regression equation proposed by (Aerens et al., 2010), as expressed by *Equation* (1).

$$F_{zs} = 0.0716\, R_m t^{1.57} d^{0.41} \Delta h^{0.09} \psi cos\, \psi \tag{1}$$

Where Δh is the scallop height defined as $\Delta h = \frac{\Delta z^2}{4d} sin^2(\psi)$. A good agreement between the two sets of results has been found with a relative error less than 4%. The force components exhibit an initial increase from the onset of deformation until it reaches a stabilization regime where it approximately becomes constant with small fluctuations around 600 N until the operation's completion. While F_x and F_y display similar magnitudes and sinusoidal shapes with a maximum magnitude $F_{max} = 300$ N. The force in the axial direction has shown a dominance compared to the components in the in-plane (x, y). This behaviour can be explained the significance of this force to induce the through-thickness deformation as indicated by (Jackson & Allwood, 2009).

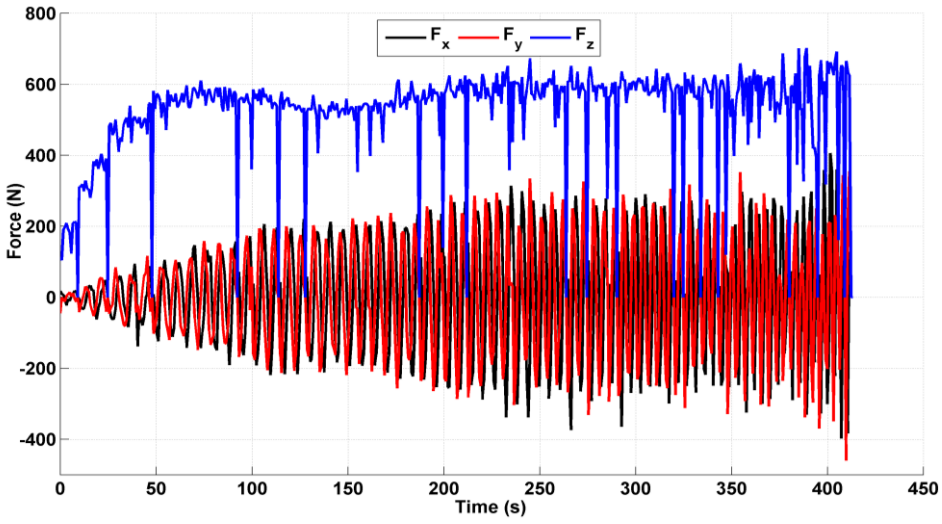

Figure 5. *Numerical results for the forming forces components F_x, F_y, and F_z during SPIF*

5.1. Plastic strain deformation

As the deformation in single point incremental sheet metal forming is more complex compared to conventional sheet metal forming, the evolution of the equivalent plastic strain in three distinct regions, denoted as A, B, and C (see *Figure 6*) was tracked in the manufactured cone as illustrated in *Figure 7*. The strain history shows a gradual increase as a function of the forming tool's movement in the z-direction. The stepwize increase in the strain indicates that the material undergoes plastic deformation only when the tool is in contact moves with the element; otherwise, the strain remains unchanged when

the punch moves away. Moreover, the equivalent plastic strain is higher in region (A) compared to the intermadiate region (B). However, the elements neighbouring region (C) exhibit lower deformation, making this area the safest zone regarding damage initiation. Quantitatively, the PEEQ values reach 2.82, 2.08, and 0.9 for the regions A, B, and C respectively.

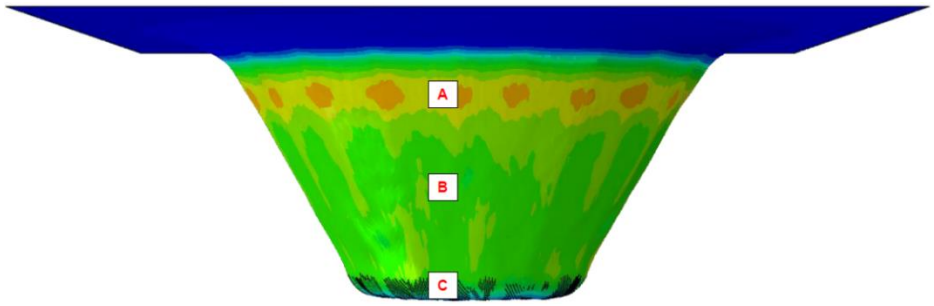

Figure 6. *Labelled distinct regions in the formed part*

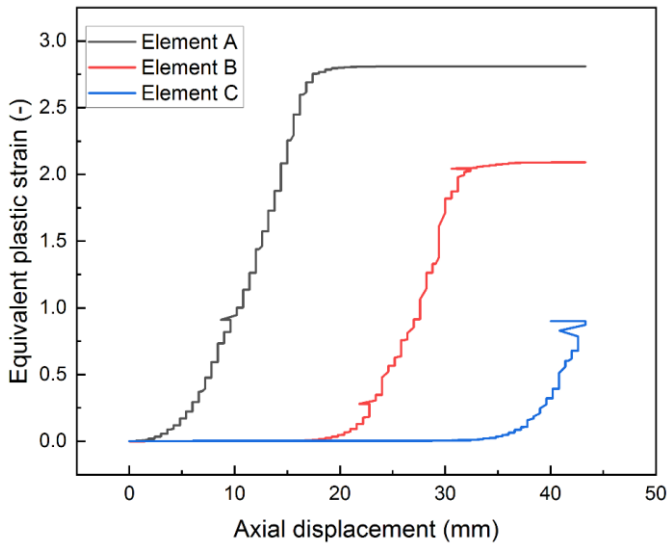

Figure 7. *Evolution of the equivalent plastic strain in distinct deform regions*

6. Conclusions

In the current research investigation, a finite element model has been developed to study the deformation mechanism in SPIF, after validating the results using an empirical equation for calculating the forming force in the steady-state regime. The axial forming force was found to have the highest magnitude compared to other two components in the radial and circonferential directions. Furthermore, the results revealed that the deformation state in SPIF is inhomogeneous. Particularly, the transition region near the outer diameter of the formed cone shape exhibited has the highest equivalent plastic strain, indicating its susceptibility to fracture.

References

[1] Aerens, R., Eyckens, P., Van Bael, A., Duflou, J. R. (2010). Force prediction for single point incremental forming deduced from experimental and FEM observations. *The International Journal of Advanced Manufacturing Technology*, 46 (9–12), 969–982. **https://doi.org/10.1007/s00170-009-2160-2**

[2] Ai, S., Long, H. (2019). A review on material fracture mechanism in incremental sheet forming. *The International Journal of Advanced Manufacturing Technology*, 104 (1), 33–61. **https://doi.org/10.1007/s00170-019-03682-6**

[3] Bensaid, K., Souissi, R., Boulila, A., Ayadi, M., Fredj, N. B. (2023). Numerical investigation of incremental forming process of AISI 304 stainless steel. *Ironmaking & Steelmaking*. **https://doi.org/10.1080/03019233.2022.2099695**

[4] Dakhore, N. P., Sonawane, D. B. U., Ghadmode, M. M. (2022). *Experimental Investigation of AA5052 in Single Point Incremental Forming Using Dynamic Tool Condition*. **https://doi.org/10.46254/IN02.20220378**

[5] Dewangan, Y. K., Gupta, A., Bandyopadhyay, K., Faye, A., Lee, M.-G. (2025). Incorporation of anisotropy for the failure prediction of AA6061 during SPIF process. *The International Journal of Advanced Manufacturing Technology*, 136 (1), 279–296. **https://doi.org/10.1007/s00170-024-14017-5**

[6] Emmens, W. C., Sebastiani, G., & van den Boogaard, A. H. (2010). The technology of Incremental Sheet Forming—A brief review of the history. *Journal of Materials Processing Technology*, *210*(8), 981–997. **https://doi.org/10.1016/j.jmatprotec.2010.02.014**

[7] Guo, W., Guo, W., Gao, F., Mo, P. (2013). Innovative group-decoupling design of a segment erector based on G F set theory. *Chinese Journal of Mechanical Engineering*, 26 (2), Article 2. **https://doi.org/10.3901/CJME.2013.02.264**

[8] Habbachi, M., Baksa, A. (2024). Numerical modelling and experimental investigation of incremental sheet metal forming of Aluminum Alloy Al 3003-O. *Journal of Physics: Conference Series*, 2848 (1), 012006. **https://doi.org/10.1088/1742-6596/2848/1/012006**

[9] Jackson, K., Allwood, J. (2009). The mechanics of incremental sheet forming. *Journal of Materials Processing Technology*, 209 (3), 1158–1174. **https://doi.org/10.1016/j.jmatprotec.2008.03.025**

[10] Jeswiet, J., Micari, F., Hirt, G., Bramley, A., Duflou, J., Allwood, J. (2005). Asymmetric single point incremental forming of sheet metal. *CIRP Annals*, 54 (2), 88–114. **https://doi.org/10.1016/S0007-8506(07)60021-3**

[11] Kumar, G., Maji, K. (2021). Investigations into enhanced formability of AA5083 aluminum alloy sheet in single-point incremental forming. *Journal of Materials Engineering and Performance*, 30 (2), 1289–1305. **https://doi.org/10.1007/s11665-021-05455-3**

[12] Maaß, F., Hahn, M., Tekkaya, A. E. (2022). Setting residual stresses in tensile stress-superposed incremental sheet forming. *Key Engineering Materials*, 926, 655–662. The 25th International Conference on Material Forming. **https://doi.org/10.4028/p-232uip**

[13] Park, J.-J., Kim, Y.-H. (2003). Fundamental studies on the incremental sheet metal forming technique. *Journal of Materials Processing Technology*, 140 (1), 447–453. **https://doi.org/10.1016/S0924-0136(03)00768-4**

[14] Racz, S. G., Breaz, R. E., Tera, M., Gîrjob, C., Biriș, C., Chicea, A. L., Bologa, O. (2018). Incremental forming of titanium Ti6Al4V alloy for cranioplasty plates—Decision-making process and technological approaches. *Metals*, 8 (8), Article 8. **https://doi.org/10.3390/met8080626**

[15] Sasso, M., Callegari, M., Amodio, D. (2008). Incremental forming: An integrated robotized cell for production and quality control. *Meccanica*, 43 (2), 153–163. **https://doi.org/10.1007/s11012-008-9124-8**

[16] Shrivastava, P., Tandon, P. (2019). Microstructure and texture based analysis of forming behavior and deformation mechanism of AA1050 sheet during Single Point Incremental Forming. *Journal of Materials Processing Technology*, 266, 292–310. **https://doi.org/10.1016/j.jmatprotec.2018.11.012**

[17] Vihtonen, L., Puzik, A., Katajarinne, T. (2008). Comparing two robot assisted incremental forming methods: Incremental forming by pressing and incremental hammering. *International Journal of Material Forming*, 1 (1), 1207–1210. **https://doi.org/10.1007/s12289-008-0158-1**